Nuclear Medicine Communications (2003) 24(5):503-511.

Estimation of fractional liver uptake and blood retention of 99mTc-DTPA -galactosyl human serum albumin: an application of a simple graphical method to dynamic SPECT.

Shuke, Noriyuki ; Aburano, Tamio ; Okizaki, Atsutaka ; Zhao, Chunlei ; Nakajima, Kenichi ; Yokoyama, Kunihiko ; Kinuya, Seigo ; Watanabe, Naoto ; Michigishi, Takatoshi ; Tonami, Norihisa

Estimation of Fractional Liver Uptake and Blood Retention of Tc-99m-DTPA-Galactosyl Human Serum Albumin: An Application of Simple Graphical Method to Dynamic SPECT.

Noriyuki Shuke, M.D.*
Tamio Aburano, M.D.*
Atsutaka Okizaki, M.D.*
Chunlei Zhao, M.D.*
Kenichi Nakajima, M.D.**
Kunihiko Yokoyama, M.D.**
Seigo Kinuya, M.D.**
Naoto Watanabe, M.D.***
Takatoshi Michigishi, M.D.**
Norihisa Tonami, M.D.**

Department of Radiology*, Asahikawa Medical College,
Asahikawa, Department of Nuclear Medicine**, Kanazawa University, Kanazawa, and
Department of Radiology***, Toyama Medical and Pharmaceutical University,
Toyama, Japan.

Address for correspondence:

Noriyuki Shuke, MD.
Department of Radiology, Asahikawa Medical College,
2-1 Midorigaoka-Higashi, Asahikawa, Hokkaido 078-8510, Japan
Phone: +81-(166) 68-2572
FAX : +81-(166) 68-2579

Running Title: Estimation of Tc-99m GSA liver uptake

Key words: Tc-99m galactosyl human serum albumin, liver uptake, hepatic function

Summary

The objective of this study was to investigate clinical utility of a graphical method for estimating liver uptake and blood retention of Tc-99m-DTPA-galactosyl human serum albumin (Tc-99m GSA) using dynamic SPECT data. Under the following two assumptions on the kinetics of Tc-99m GSA: 1) Tc-99m-GSA distributes only between blood and liver; 2) no Tc-99m-GSA metabolism during observation period, a plot of liver counts versus cardiac blood pool counts should be theoretically on a straight line. From the slope and y-intercept of a regression line, coefficients for converting count-based liver and blood pool data to % injected dose (%ID) can be calculated. The applicability of this method was tested on dynamic SPECT data from 30 patients with liver dysfunction. To validate this method, plasma concentrations (%ID/ml plasma) at 6, 15 and 30 minutes after the injection were estimated by this method and compared with the measured ones. To investigate clinical significance of % liver uptake, % liver uptake obtained by this method was compared with the results of conventional liver function tests including serum albumin, hepaplastin test, prothrombin time and indocyanine green clearance. In every data set, a plot of liver counts to cardiac blood pool counts was fitted well by a straight line ($p<0.00001$). Estimated plasma concentrations by this method showed good correlations with the measured ones at 6, 15 and 30 min after the injection ($r=0.748$, 0.838, 0.875, respectively, $p<0.0001$). The liver uptake determined by this method showed good correlations with the results of conventional hepatic function tests ($p<0.002$). The graphical method could provide accurate estimate of %ID of Tc-99m GSA in the blood without blood sampling. The liver uptake determined by this method could be a simple but useful quantitative indicator of hepatic function.

Introduction

The asialoglycoprotein receptor, which resides on the surface of hepatocyte, is thought to be responsible for the metabolism of serum glycoprotein [1]. The receptor density in the liver is closely related to the hepatocellular function [2]. In the field of nuclear medicine, the development of Tc-99m labeled neoglycoalbumin (Tc-99m NGA) for in vivo use enabled the direct imaging of the liver asialoglycoprotein receptor. In conjunction with visual evaluation of the receptor image, using time-activity curves of liver and cardiac blood pool, kinetic model analyses have been performed to estimate the hepatic receptor density [3-5]. In the first step of quantitative analysis of imaging data, it is usually necessary to calibrate count-based data recorded by digital gamma camera system to the concentration-based or fractional dose-based data expressed with a general unit such as percentages of the injected dose (%ID). Not only for further quantitative model analysis, fractional uptake in the liver (% liver uptake) in itself can be useful for the evaluation of hepatic function [6, 7]. Standard procedures for this calibration are accomplished by determination of calibration coefficients from measured blood radioactivity and the corresponding blood pool count or from camera-based organ uptake and corresponding liver counts on the images [3, 8]. As a simple alternative to these calibration procedures, a graphical method for estimating the calibration coefficient by a simple linear regression analysis of the liver and cardiac blood pool time-activity data has been developed [9-11]. In this study, the applicability of this method to dynamic SPECT data was tested and the clinical significance of the % liver uptake obtained by this method was investigated in relation to the hepatic function,

using data from 30 patients who underwent dynamic liver SPECT with Tc-99m-DTPA-galactosyl human serum albumin (Tc-99m GSA).

Methods

Radiopharmaceutical

Radiolabeled neoglycoalbumin used in this study was Tc-99m-DTPA-galactosyl human serum albumin (Tc-99m-GSA, Nihon Mediphysics, Nishinomiya, Japan), which was a radiolabeled synthetic analog of endogenous asialoglycoprotein. Tc-99m-GSA (MW.76000) has about 33 galactose residues and DTPA conjugated for chelating Tc-99m. Tc-99m-GSA has moderate affinity toward the asialoglycoprotein receptor residing at the plasma membrane of hepatocyte and is used for the assessment of liver function through the receptor-ligand binding [12, 13]. Tc-99m-GSA was provided in a labeled form with more than 98% specific activity.

Patients

A total of 30 patients with liver dysfunction (Female: 10, Male: 20) aged 35-71 years old (mean ± sd: 59 ± 9), consisting of 23 chronic liver diseases and 7 metastatic liver tumors, were studied. The patients were classified into three groups according to the degree of liver dysfunction (A: mild, B: moderate, C: severe) on Child's criterion [14]. Eleven patients were classified into group A, 10 patients into group B and 9 patients into group C.

Dynamic SPECT data acquisition

Dynamic SPECT studies were performed using a triple-headed rotating gamma camera system equipped with low energy general-purpose collimators and a dedicated data processing unit (GCA9300A and GMS550, Toshiba Medical, Tokyo, Japan). The in-plane spatial resolution of this gamma camera system was 14 mm FWHM. After

overnight fasting, setting a patient in a supine position so that the liver and lower part of the heart could be within the field of view of the detectors, Tc-99m-GSA (185 MBq/3mg) was injected intravenously as a bolus. After confirming that the entire liver was covered by the detectors' view, dynamic SPECT data acquisition was started one minute after the injection and continued for 30 rotations in a 120-degree back and forth continuous rotation mode with an acquisition time of 1 minute per each rotation. In each rotation, 90 projection data (30 projections/detector) were recorded in a 64 x 64 matrix (pixel size: 6.4mm x 6.4 mm). The SPECT image reconstruction was performed with a filtered back-projection method using a ramp filter after pre-processing with a Butterworth filter (cutoff frequency 0.41 cycle/cm, order 8) to obtain 6.4 mm thick transaxial images. Attenuation and scatter corrections were not performed.

By a threshold percentage (42%) to the maximum voxel count in the liver, the border of the liver was determined on the reconstructed trans-axial images obtained from the 30th rotation in which the liver was delineated most clearly. On the other hand, to obtain time-activity data of blood, a region of interest (ROI) was roughly drawn over the cardiac blood pool on the transaxial slice obtained from the first rotation in which blood pool activity was most prominent. A threshold percentage of 70 % to the maximum voxel count in the ROI was used for determining the edge of the cardiac blood pool. The time-activity curves of cardiac blood pool and whole liver were then generated based on these ROIs.

During SPECT data acquisition, peripheral vein blood sampling (3 ml each) was performed 6, 15, and 30 min after the injection. After centrifugation of the sampled blood, 0.5 ml of plasma was aliquoted into plastic test tubes in duplicate from each sample. Together with the diluted solution of the injected standard, radioactivity of the

plasma was counted on a well-type scintillation gamma counter (ARC500, Aloka, Tokyo, Japan) to calculate plasma concentration of Tc-99m GSA in a unit of % injected dose/ml plasma. The actual injected dose was determined by counting the radioactivity of pre- and post-injection syringe on a dose calibrator (IGC3, Aloka, Tokyo, Japan). A calibration coefficient for converting radioactivity measured on the curie meter to that on the well-type scintillation counter was determined by counting a standard solution on both measuring instruments.

Graphical method for conversion of gamma camera counts to % injected dose

Under the following assumptions on Tc-99m-GSA kinetics, 1) distribution only between blood and liver, 2) No metabolism nor excretion from the liver or body during observation period, the following linear relationship between liver and cardiac blood pool radioactivity can be formulated after the attainment of homogenous tracer distribution in the blood:

c•L(t)+Vc•H(t)=Do --------(Eq. 1)

where **H(t)** and **L(t)** represent counts in cardiac blood pool ROI and whole liver ROI at arbitrary time **t**. **Do** is total injected dose. **Vc** is extrahepatic blood volume scaled by the ROI volume of the cardiac blood pool, and **c** is a correction coefficient to correct a difference in counting sensitivity of gamma camera between liver and cardiac blood pool. The first term of the left side of **Eq. 1** (**c•L(t)**) thereby means Tc-99m-GSA amount in the liver scaled by the same detector sensitivity to cardiac blood pool. The second term (**Vc•H(t)**) means Tc-99m GSA amount in the extrahepatic blood. If there is no metabolism, the sum of the amounts in the liver and extrahepatic blood should equal

to the injected dose (**Do**) at any time**.** Thus, the linear relationship described in Eq. 1 holds as far as the two assumptions described above are satisfied. Solving Eq.1 for **L(t)**, following linear equation can be obtained (Eq. 2).

L(t)=-Vc/c•H(t)+Do/c -------(Eq. 2)

The Eq. 2 means that a plot of liver counts to cardiac blood pool counts should be on a straight line with a negative slope. A reciprocal of the y-intercept (**c/Do**) is a coefficient for converting liver counts to fractional liver uptake. Dividing the absolute value of the slope (**Vc/c**) by the y-intercept (**Do/c**), the obtained quotient (**Vc/Do**) is a coefficient for converting cardiac blood pool counts to fractional dose in the extra-hepatic blood. In this way, the two coefficients necessary for converting counts in the liver and cardiac blood pool ROIs to the respective fractions of the injected dose (%ID) can be determined from the results of simple linear regression.

In applying this method to the dynamic SPECT data, 27 data points obtained from the 4th to 30th rotations, were used for linear regression. Since homogeneous distribution of the tracer in the blood could not be attained in a few minutes after the injection, the first three data points were omitted.

Reproducibility and validation of the graphical method

To test the effect of ROI size on the reproducibility of this method, various threshold percentages to the maximum voxel count were used to determine the boundaries of liver and cardiac blood pool in 1 patient. Threshold percentages of 20, 30, 40, 50% were used for the liver, and 0, 40, 60, 80% were used for the cardiac blood pool. Based on these ROIs, time-activity curves were generated. Using every

combination of the liver and cardiac blood pool time-activity curves, the graphical method was performed to obtain the coefficients. Using the obtained coefficients, %ID in the liver at 15 min and 30 min post-injection (LU15 and LU30) were calculated for each combination and the reproducibility was tested.

To validate the method, plasma concentration of Tc-99m GSA estimated by this method was compared with the calculated one from the sampled plasma data. The fraction of Tc-99m-GSA existed in extrahepatic blood at arbitrary time was calculated by multiplying the coefficient for cardiac blood pool ROI (**Vc/Do**) by actual counts in the ROI. On the other hand, patient's total blood volume (TBV) was estimated from patients' weight and height based on the following equations (Eq. 3, 4) that were originally proposed by Nadler and modified for Japanese by Fujita [15, 16]. Based on the estimated total blood volume and measured hematocrit, patients' total plasma volume was estimated (Eq. 5).

$$TBV\ (\text{for male}) = (0.0236H^{0.725}\ W^{0.425} - 1.229) \quad \text{---(Eq. 3)}$$

$$TBV\ (\text{for female}) = (0.0248H^{0.725}\ W^{0.425} - 1.954) \quad \text{---(Eq. 4)}$$

$$TPV = TBV(1-Ht) \quad \text{---(Eq. 5)}$$

In Eq. 3-5, TBV, H, W, TPV and Ht represent total blood volume (*l*), height (m), weight (kg), total plasma volume (*l*), and hematocrit, respectively.

Assuming intrahepatic plasma was 10 percent of total plasma volume [17], extrahepatic plasma volume was approximated to be 90 percent of total plasma volume. Dividing the estimated %ID of Tc-99m GSA in the extrahepatic blood by the estimated extrahepatic plasma volume, plasma concentration of Tc-99m GSA was estimated in a unit of %ID/ml plasma. The estimated Tc-99m GSA plasma concentrations at 6, 15,

and 30 min after the injection were compared with the calculated ones from the measured radioactivity of sampled venous plasma and the injected standard.

Clinical significance of Tc-99m-GSA liver uptake

As the simplest quantitative index for liver asialoglycoprotein receptor density, Tc-99m-GSA liver uptake at 15 min after injection (LU15) was reported to be valuable in evaluation of hepatic function [7]. LU15 obtained by this method was therefore compared with the results of the various hepatic function tests and its clinical significance was investigated. The conventional hepatic function tests, including serum albumin, hepaplastin test, prothrombin time, indocyanine green clearance, total bilirubin and choline esterase, were used for the comparison. Liver uptake at 6 min and 30 min (LU6 and LU30) were also calculated and compared with LU15 in relation to hepatic function.

Results

Dynamic SPECT and the graphical method

In all cases, both liver and cardiac blood pool were clearly visualized on dynamic SPECT images. An example is shown in Fig. 1. The Cardiac blood pool activity, which was prominent in the initial phase, declined promptly in process of time. On the other hand, Liver activity was faint in the initial phase, but the tracer gradually shifted to the liver, delineating it clearly in the later phase. Using dynamic SPECT, the tracer kinetics

could be evaluated three-dimensionally and precise liver and cardiac blood pool time-activity curves could be obtained.

From the dynamic SPECT images, time activity curves of the liver and cardiac blood pool were obtained and used for the graphical analysis. In all 30 cases, plot of liver counts over cardiac blood pool counts was fitted well by the linear equation (Eq. 2). Correlation coefficients ranged from -0.725 to -0.997 (mean ± sd.: -0.973±0.050, $p<0.00001$ in all cases).

Effect of ROI size on the reproducibility

The results of boundary determination with the various threshold percentages for whole liver and cardiac blood pool are shown in Fig. 2. The ROI sizes of liver and cardiac blood pool changed noticeably, depending on the threshold percentage. The ROI volumes ranged from 27 to 167 ml for the cardiac blood pool and from 458 to 1147 ml for the whole liver. Generated time-activity curves and the examples of graphical plots are shown in Fig. 3. In every combination of the liver and cardiac blood pool time-activity curves, a plot of liver counts over cardiac blood pool counts was on a straight line and fitted well by the linear equation (Eq. 2). Using coefficients obtained from the slopes and y-intercepts of the fitted lines, % liver uptakes at 15 min after the injection were calculated for each combination. The results are summarized in Table.1-A, B. Although the ROI volumes of both liver and cardiac blood pool changed considerably depending on the threshold percentage, the estimated uptake was not changed so much. Constants of variation of the estimated liver uptakes were smaller than 5%, showing good reproducibility.

Comparison with the measured plasma concentration

Relationship between estimated plasma Tc-99m-GSA concentration by the graphical method and measured one is shown in Fig. 4. At 6, 15 and 30 min after the injection, estimated concentrations were in good agreement with calculated ones, showing significant correlations ($r=0.748$, $r=0.838$, $r=0.875$, respectively, $p<0.0001$ at all time points).

Clinical significance of Tc-99m-GSA liver uptake

Estimated %liver uptake at 6 min, 15 min, and 30 min post-injection (LU6, LU15, LU30) ranged from 19 to 63 %, from 24 to 82%, and from 30 to 87 %, respectively. At all time points, %liver uptake showed statistically significant correlations with the various hepatic function tests (Table 2), but there was not much difference in the significance level of correlations among time points. Compared with the Child's classification, however, LU6 showed the most significant difference in discriminating between mild dysfunction (group A) and moderate (group B), and the significance level of difference became smaller in LU15 and smaller still in LU30, and thus decreased in the order of time. In discriminating between moderate dysfunction (group B) and severe (group C), LU6, LU15 and LU30 showed the difference of similar significance.

Discussion

The graphical method described in this paper has been developed for conversion of count-based liver and blood data obtained from dynamic images to standardized fractional dose-based data. For this purpose, gamma camera-based liver uptake is commonly calculated from counts of an organ ROI and injected dose determined by

syringe counting or whole body counting [6-8]. Although this camera-based organ uptake is simple to implement, the uptake value obtained by this method could be influenced directly by ROI size. Furthermore, any error in the syringe counting would also affect the outcome significantly. These potential sources of error in determining organ uptake are theoretically avoided by using the graphical method, which is relatively independent of ROI size and does not require syringe counting. In return for these advantages, the graphical method requires the two assumptions described in the method section. Since Tc-99m GSA has a similar molecular size to albumin which is a typical intravascular tracer, the first assumption that the distribution of the tracer is restricted to blood and liver could be acceptable in the majority of clinical cases. The second assumption of no excretion or metabolism of neoglycoalbumin during observation period could hold true at least first 30 min after the injection, since excreted bile activity was never seen to a significant degree in the dynamic SPECT images in this study. In addition, these assumptions were already used by other investigators in constructing the kinetic models of radiolabeled neoglycoalbumin [3, 11, 18], and seemed to have no serious adverse effect on the model consistency. Our results, in which highly significant liner fitting was obtained based on these assumptions, also proved the correctness of these assumptions.

As for time-blood concentration profile of the tracer, which is also necessary for kinetic modeling analysis, blood concentration measured at certain time point is usually used to calibrate time-activity curve obtained from cardiac blood pool ROI [18]. As an alternative to this blood sampling method, fractional dose in a blood compartment at arbitrary time can be estimated by normalizing blood pool counts by the interpolated initial blood pool counts at time zero [19]. For this interpolation, bolus input assumption and a particular kinetic model are necessary to obtain theoretical blood

time-activity curve. In practical cases, however, tracer may not be injected as a good bolus, moreover, homogenous distribution in a blood compartment may not be attained soon after the injection. These factors may affect the estimated initial blood pool counts more or less. Furthermore, since multi-exponential function is usually used as a theoretical curve for blood time-activity profile, nonlinear regression is necessary to determine initial blood pool counts. In contrast to these methods, the graphical method does not require blood sampling or nonlinear regression. Instead of nonlinear curve fitting, only simple linear regression is required. Along with these features, it should be emphasized that the graphical method has excellent reproducibility independent of ROI size. In these respects, the graphical method would be suitable for routine clinical use to estimate fractional dose in the liver and blood.

The limitation of the method may, however, arise when applying the method in patients with very severe liver dysfunction in whom liver uptake of the tracer is expected to be very low. To put it an extreme way, if the shift of the tracer from blood to liver does not take place, the plot converges to one point and slope and y-intercept could not be determined. Therefore, in case of extremely severe hepatic dysfunction, it might be difficult to determine the regression line with a small error. If the regression lines showed poor fit, obtained results should be treated with due caution.

Considering the nonlinear kinetics of neoglycoalbumin, liver uptake of this tracer may not be an ideal quantitative index for the receptor density. It may be affected by several factors including injected dose and patient’s body size. However, conventional indexes such as gamma camera-based liver uptake and the count ratio of liver to blood pool have been used in evaluation of asialoglycoprotein receptor imaging [6, 7, 20]. Although simple and limited by several factors, these indexes are recognized as useful indicators of hepatic functional reserve in the past clinical studies. In our data, liver

uptake obtained by the graphical method also showed good correlation with the results of conventional hepatic function tests, indicating its clinical usefulness.

In comparison with the Child's classification, the significance level of the difference in liver uptake (LU6, LU15, LU30) between mild dysfunction (group A) and moderate (group B) decreased in order of time, showing best discrimination by LU6. In discriminating between moderate dysfunction (group B) and severe (group C), LU6, LU15 and LU30 showed the difference of similar significance, not in order of time. The reason for these results may be explained by the injected dose and the nonlinear kinetics of the tracer. The injected dose used in this study (3 mg of Tc-99m GSA) amounts to about 40 n moles. This dose was not enough to saturate the receptor in normal liver, which was about several hundred n moles in amount [3]. With this dose, it might be difficult to distinguish between mild dysfunction and moderate by the late phase liver uptake (LU15 and LU30), since the receptor amount in this range of hepatic dysfunction might be more than 40 n mole and the late phase liver uptake might be limited not by the total liver receptor amount but by the total ligand amount. On the contrary, the early phase liver uptake (LU6) was able to discriminate between mild dysfunction and moderate more significantly than the late phase uptake. This result could be explained as follows. In the early phase, the fraction of the receptor bound to the total liver receptor could be negligible and linear uptake could be assumed. In this situation, the early phase liver uptake reflects liver uptake rate, which is theoretically determined by the product of free receptor density, and second order forward binding rate constant. On the other hand, late phase uptake may be limited by the total receptor or total ligand amounts, depending on patient’s total liver receptor amount. For these reasons, early phase liver uptake was probably more sensitive than late phase liver uptake in differentiating mild hepatic dysfunction. Apart from liver uptake, other linear

parameters representing early phase liver uptake such as liver clearance calculated by Patlak plot could be used as alternatives to the receptor amount determined by nonlinear model analysis [21]. Using the standardized data after the graphical analysis, further simple approaches to regional evaluation of the receptor amount and hepatic blood flow could be implemented in Tc-99m GSA dynamic SPECT [22].

Conclusion

The graphical method could provide accurate estimate of %ID of Tc-99m GSA in the blood without blood sampling. The liver uptake determined by this method could be a simple but useful quantitative indicator of hepatic function.

REFERENCES

1. Ashwell G, Morell AG. The role of surface carbohydrates in the hepatic recognition and transport of circulating glycoproteins. *Adv Enzymol Relat Areas Mol Biol* 1974; 41: 99-128.
2. Sawamura T, Kawasato S, Shiozaki Y, Sameshima Y, Nakada H, Tashiro Y. Decrease of a hepatic binding protein specific for asialoglycoproteins with accumulation of serum asialoglycoproteins in galactosamine-treated rats. *Gastroenterology* 1981; 81: 527-533.
3. Vera DR, Stadalnik RC, Trudeau WL, Scheibe PO, Krohn KA. Measurement of receptor concentration and forward-binding rate constant via radiopharmacokinetic modeling of technetium-99m-galactosyl-neoglycoalbumin. *J Nucl Med* 1991; 32: 1169-1176.
4. Kudo M, Vera DR, Trudeau WL, Stadalnik RC. Validation of in vivo receptor measurements via in vitro radioassay: technetium-99m-galactosyl-neoglycoalbumin as prototype model. *J Nucl Med* 1991; 32: 1177-1182.
5. Ha-Kawa SK, Tanaka Y, Hasebe S et al. Compartmental analysis of asialoglycoprotein receptor scintigraphy for quantitative measurement of liver function: a multicentre study. *Eur J Nucl Med* 1997; 24: 130-137.
6. Sugai Y, Komatani A, Hosoya T, Yamaguchi K. Response to percutaneous transhepatic portal embolization: new proposed parameters by 99mTc-GSA SPECT and their usefulness in prognostic estimation after hepatectomy. *J Nucl Med* 2000; 41: 421-425.

7. Koizumi K, Uchiyama G, Arai T, Ainoda T, Yoda Y. A new liver functional study using Tc-99m DTPA-galactosyl human serum albumin: evaluation of the validity of several functional parameters. *Ann Nucl Med* 1992; 6: 83-87.

8. Ha-Kawa SK, Tanaka Y. A quantitative model of technetium-99m-DTPA-galactosyl-HSA for the assessment of hepatic blood flow and hepatic binding receptor. *J Nucl Med* 1991; 32: 2233-2240.

9. Shuke N, Aburano T, Nakajima K et al. Proposal of a graphical method for the estimation of asialoglycoprotein receptor amount in the liver using Tc-99m-DTPA-galactosyl human serum albumin (abstract). *J Nucl Med* 1994; 35(suppl): 172.

10. Ishikawa Y, Sato J, Shuke N et al. Simple method for estimating fractional liver uptake and blood concentration in Tc-99m galactosyl human serum albumin liver scintigraphy (abstract). *Ann Nucl Med* 1996; 10(suppl): 59.

11. Miki K, Kubota K, Kokudo N, Inoue Y, Bandai Y, Makuuchi M. Asialoglycoprotein receptor and hepatic blood flow using technetium-99m-DTPA-galactosyl human serum albumin. *J Nucl Med* 1997; 38: 1798-1807.

12. Kudo M, Washino K, Yamamichi Y, Ikekubo K. Synthesis and radiolabeling of galactosyl human serum albumin. *Methods Enzymol* 1994; 247: 383-394.

13. Torizuka K, Ha-Kawa SK, Ikekubo K et al. Phase I clinical study on 99mTc-GSA, a new agent for functional imaging of the liver. *Jpn J Nucl Med* 1991; 28: 1321-1331.

14. Child CG, Turcotte JG. Surgery and portal hypertension. in: Child CG, ed. The liver and portal hypertension. Philadelphia: W. B. Saunders, 1964: 1-85.

15. Nadler S, Hidalgo J, Bloch T. Prediction of blood volume in normal human

adults. *Surgery* 1962; 51: 224-232.

16. Fujita T. A review on measurements of the body fluids. *Saishin Igaku* 1971; 26: 233-241.

17. Guyton A, Hall J. The liver as an organ. In: Guyton A, Hall J, eds. Textbook of medical physiology. Philadelphia: W.B. Saunders, 1996: 883-888.

18. Vera DR, Woodle ES, Stadalnik RC. Kinetic sensitivity of a receptor-binding radiopharmaceutical: technetium-99m galactosyl-neoglycoalbumin. *J Nucl Med* 1989; 30: 1519-1530.

19. Ha-Kawa SK, Suga Y, Kouda K, Ikeda K, Tanaka Y. Validation of curve-fitting method for blood retention of 99mTc-GSA: comparison with blood sampling method. *Ann Nucl Med* 1997; 11: 15-20.

20. Shiomi S, Kuroki T, Kuriyama M et al. Evaluation of fulminant hepatic failure by scintigraphy with technetium-99m-GSA. *J Nucl Med* 1997; 38: 79-82.

21. Shuke N, Aburano T, Nakajima K et al. Quantitative evaluation of regional hepatic function with Tc-99m-DTPA-galactosyl human serum albumin liver dynamic SPECT (abstract). *J Nucl Med* 1995; 36(suppl): 75.

22. Katada R, Shuke N, Saitoh Y et al. Simple kinetic analysis of 99mTc-GSA by direct integral linear least square regression method: calculation of hepatic blood flow and receptor index based on three-compartment model. *Jpn J Nucl Med* 1998; 35: 85-91.

Figure Legends

Fig. 1.

Transaxial dynamic SPECT images (1min/rotation) obtained 1 to 30 min after the injection of Tc-99m GSA (185 MBq/3mg). Each column represents the same slices at different time points and each row represents the consecutive slices from the cardiac ventricles (left) to lower liver level (right) at the same time point.

Fig.2.

Results of the determination of cardiac blood pool and liver boundaries using 4 different cutoff percentages to the maximum voxel counts. The resultant 4 transaxial images of the cardiac blood pool with the different cutoff percentages at the same cardiac ventricular level gave the volumes ranged from 27 to 167 ml (A). The resultant 4 sets of transaxial images of the liver with the different cutoff percentages gave the volumes ranged from 458 to 1147 ml (B). Each set covers entire liver from the upper (left) to the lower liver level (right).

Fig.3.

Influence of ROI size on the reproducibility of the graphical method.
Time activity curves of the cardiac blood pool (A) and liver (B) based on the boundaries determined with the 4 different cutoff percentages are quite different from each other. Based on these time activity curves, graphical method was performed. Example plots from combinations of time activity curves of cardiac blood pool (40% cutoff) and liver (20, 30, 40 and 50% cutoff) are shown (C). Obtained liver uptake at

15min post injection (LU15) showed good reproducibility regardless of the cutoff percentages for the liver and cardiac blood pool boundaries (D). Mean and constant of variation (CV) of LU15 are 36% and 3.7%.

Fig. 4.

Correlation between estimated plasma Tc-99m-GSA concentration by the graphical method and calculated one from the measured plasma radioactivity and injected dose. At 6, 15 and 30 min after the injection, estimated plasma concentrations show significant linear correlations with calculated ones (A, B and C, respectively).

Fig. 5.

Difference of liver uptake among the grades of Child's classification.
Liver uptake of Tc-99m GSA at 6, 15 and 30min post injection (LU6, 15 and 30) are plotted in relation to the disease severity according to the Child's classification (A, B and C, respectively).

Table 1.

Correlation coefficients between liver function tests and liver uptakes at 6, 15 and 30 min post injection. ICGR15 represents blood retention of indocyanine green (ICG) at 15min post injection in the ICG clearance test. Liver uptake showed significant correlations with the conventional liver function tests at all three time points.

Fig.2-B

20 % Cut Off
1147 ml

30 % Cut Off
872 ml

40 % Cut Off
681 ml

50 % Cut Off
458 ml

Fig.2-A

0 % Cut Off
167 ml

40 % Cut Off
101 ml

60 % Cut Off
67 ml

80 % Cut Off
27 ml

Fig.1

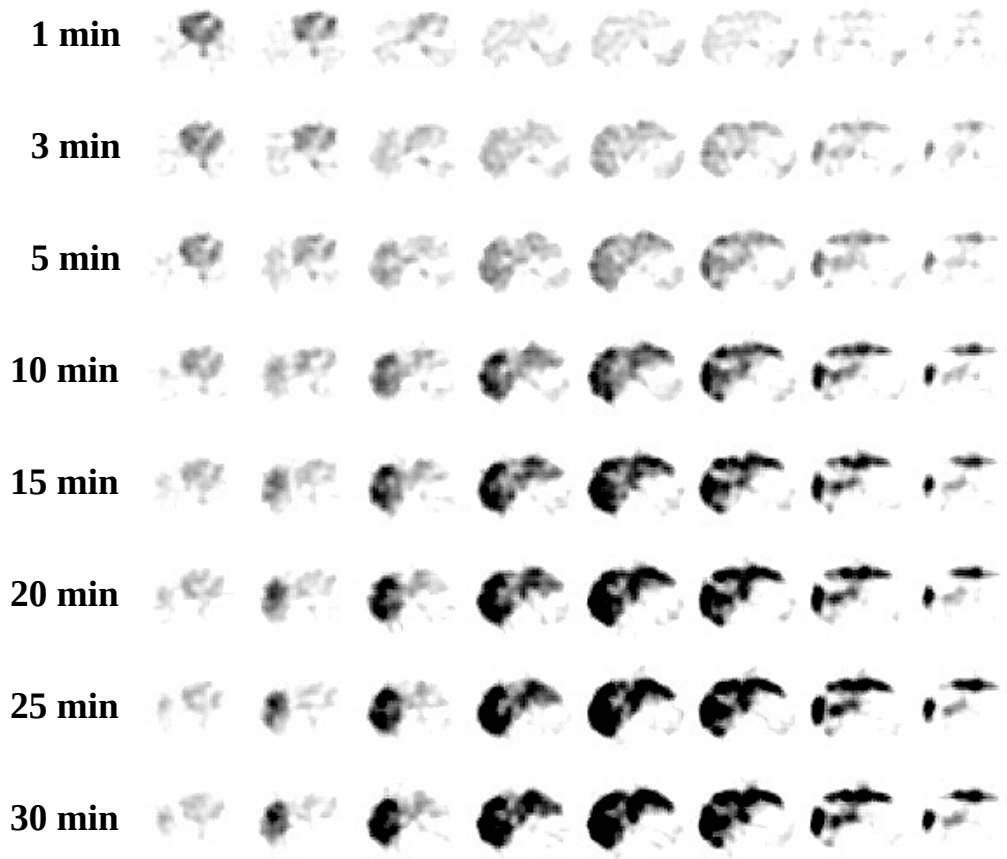

Fig.4

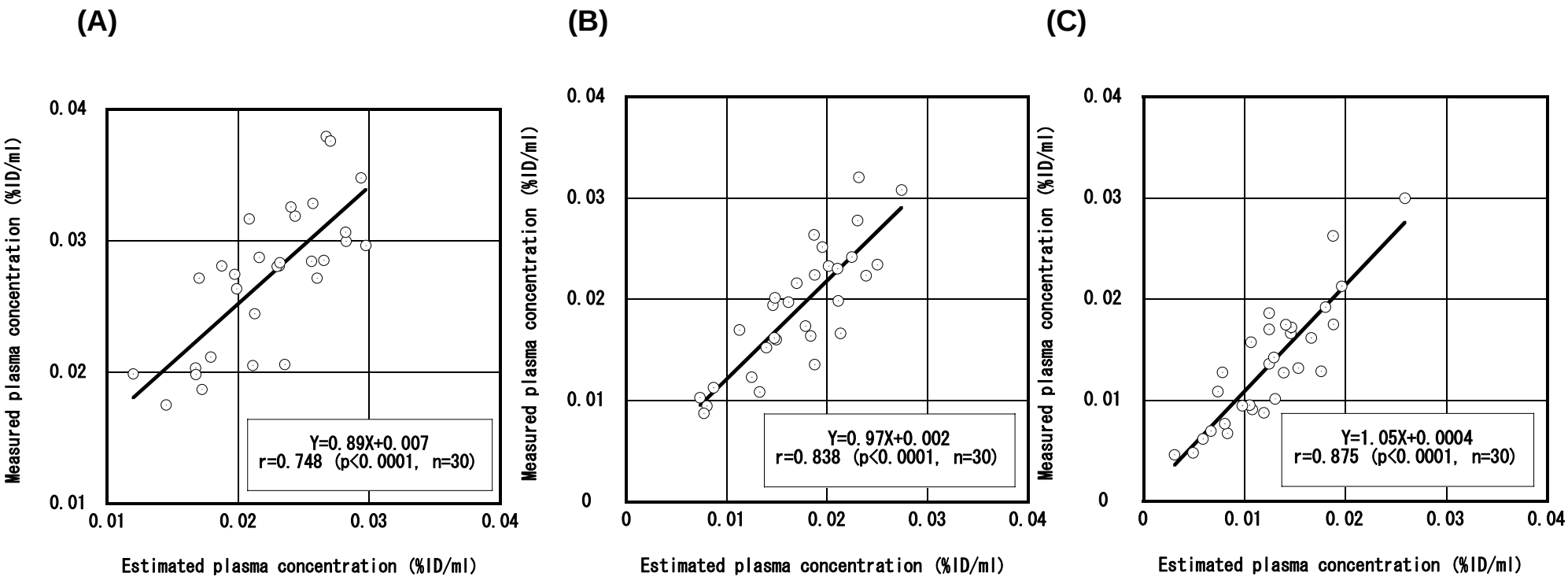
(A)
(B)
(C)
Measured plasma concentration (%ID/ml)
Estimated plasma concentration (%ID/ml)
0.04
0.03
0.02
0.01
0
Y=0.89X+0.007
r=0.748 (p<0.0001, n=30)
Y=0.97X+0.002
r=0.838 (p<0.0001, n=30)
Y=1.05X+0.0004
r=0.875 (p<0.0001, n=30)

Fig.3

(A)

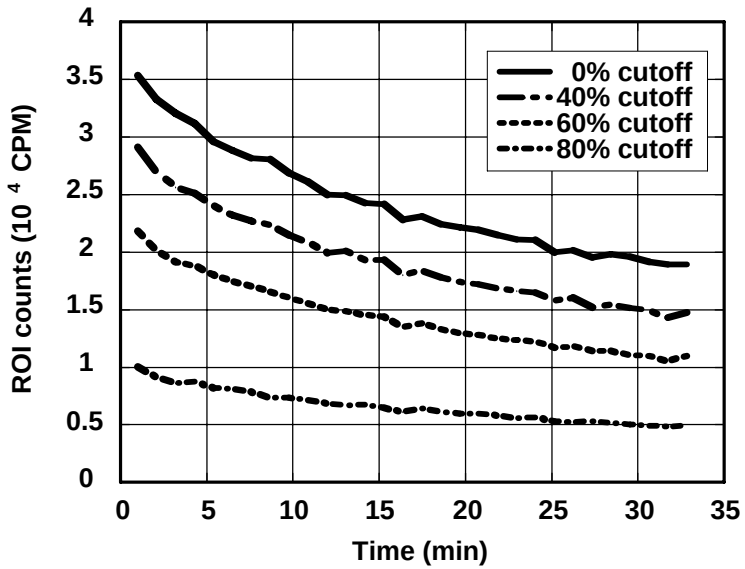

(B)

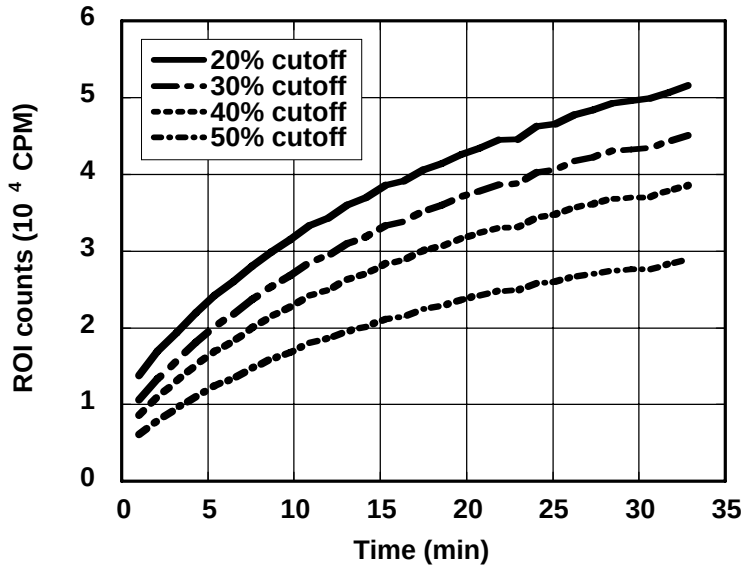

(C)

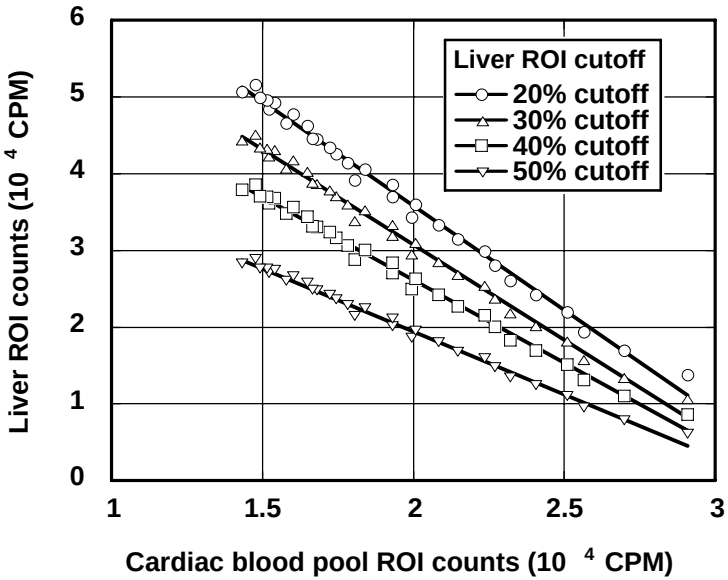

(D)

Liver ROI cutoff (%)	Cardiac blood pool ROI cutoff (%) 0	40	60	80
20	35	37	38	38
30	34	36	36	37
40	34	35	36	36
50	33	35	35	36

(Mean: 36, CV: 3.7%)

Table 1

	LU6(%)	LU15(%)	LU30(%)
Albumin (g/dl)	0.543 (p<0.002)	0.588 (p<0.001)	0.627 (p<0.001)
Hepaplastin test (%)	0.562 (p<0.001)	0.577 (p<0.001)	0.585 (p<0.001)
Prothrombin time (sec)	-0.569 (p<0.001)	-0.614 (p<0.001)	-0.646 (p<0.001)
ICGR15 (%)	-0.694 (p<0.001)	-0.637 (p<0.001)	-0.541 (p<0.002)
Total Biliirubin(mg/dl)	-0.474 (p<0.001)	-0.537 (p<0.001)	-0.592 (p<0.001)
Choline Esterase (IU/dl)	0.653 (p<0.001)	0.674 (p<0.001)	0.622 (p<0.001)

Fig.5

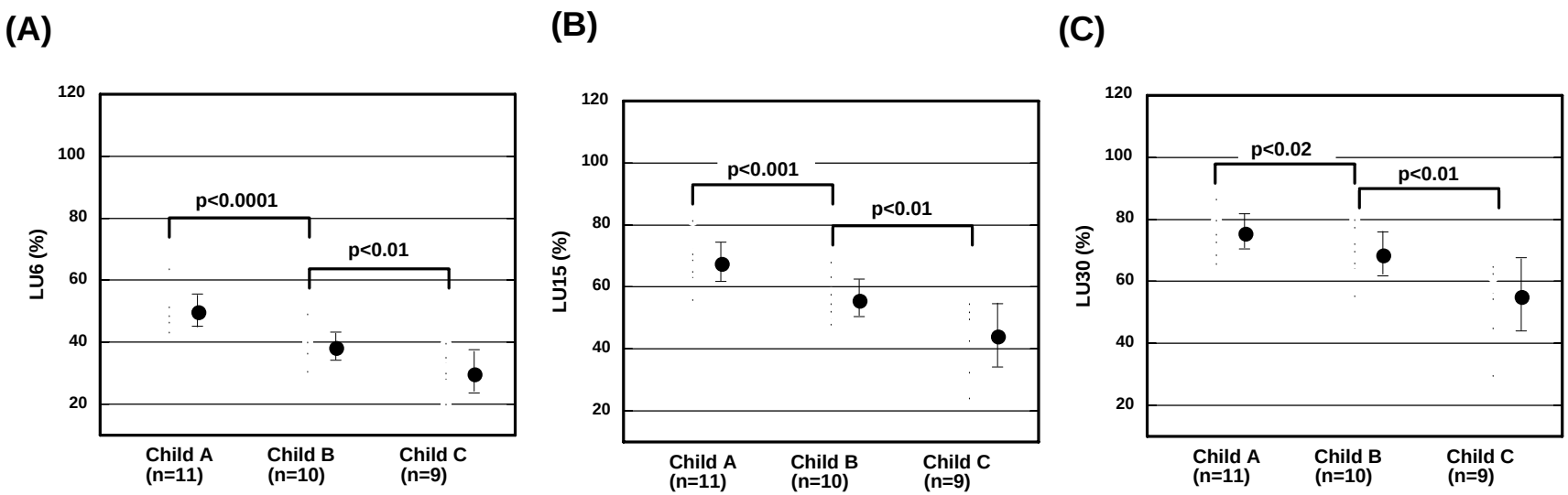
(A)
LU6 (%)
120
100
80
60
40
20
p<0.0001
p<0.01
Child A (n=11)
Child B (n=10)
Child C (n=9)
(B)
LU15 (%)
120
100
80
60
40
20
p<0.001
p<0.01
Child A (n=11)
Child B (n=10)
Child C (n=9)
(C)
LU30 (%)
120
100
80
60
40
20
p<0.02
p<0.01
Child A (n=11)
Child B (n=10)
Child C (n=9)